Determination of Nonlinear Optical Properties of MgO Nanoparticles Doped in Poly (Ether) Urethane

M. Nadafan[a], R. Malekfar[a,*] and Z. Dehghani[b]

[a]Department of Physics, Tarbiat Modares University, P.O. Box 14115-175, Tehran, I.R. Iran

[b]Faculty of Sciences, Department of Physics, University of Neyshabur, Neyshabur, I.R. Iran

(Received September 17, 2014; in final form May 10, 2015)

The third-order optical nonlinearities of poly (ether) urethane open cell (PEUOC)/MgO nanocomposites, dissolved in dimethylformamide are characterized by Z-scan technique with CW Nd:YAG laser at its second harmonic frequency of 532 nm with TEM00 Gaussian profile. The synthesized samples are also characterized by optical microscopy and scanning electron microscopy imaging. The nonlinear refractive indices and nonlinear absorption coefficients of the synthesized samples are obtained in the order of 10^{-8} cm^2/W with negative sign and 10^{-5} cm/W, respectively. The origin of optical nonlinearity in this case may be attributed due to the presence of strong saturable absorption effect. All the results suggest that the nonlinear coefficients of the synthesized samples can be controlled by nanoparticles content into PEUOC. Furthermore, the results show that PEUOC/MgO may be promising candidate for the application to optical limiting in the visible region.

DOI: 10.12693/APhysPolA.128.29

PACS: 42.65.–k

1. Introduction

In the last few decades, great efforts have been made in the field of nonlinear optics (NLO) and it has been developed as a promising area of research with wide range of potential applications [1–5]. There is considerable interest in finding materials having large yet fast nonlinearities. This interest, that is driven primarily by the search for materials for all-optical switching and sensor protection applications, concerns both nonlinear absorption (NLA) and nonlinear refraction (NLR) [6].

Among these, organic polymeric materials have advantages with considering their easy modified structures, the ability of converting them into thin films, their high laser damage thresholds, faster response time and others [7]. However, inorganic materials such as different nanoparticles play a crucial role in determining their linear and nonlinear optical properties through their surfaces, such as emission behavior and third-order optical nonlinearities [8]. The latest interests attribute to design new nanomaterial systems with improved performances such as polymer nanocomposites because of including both characteristics of organic-inorganic properties.

In the present work, we will evaluate the effects of MgO nanoparticles (NPs) in PEUOC matrix by considering its optical properties such as optical microscopy imaging and scanning electron microscopy (SEM) imaging. Furthermore, we will investigate on the third-order nonlinear optical properties of PEUOC/MgO nanocomposites by using the closed-aperture (CA) and open-aperture (OA) Z-scan techniques with the Nd:YAG laser at a 532 nm wavelength with continuous-wave (CW).

*corresponding author; e-mail: malekfar@modares.ac.ir

2. Materials

Magnesium oxide (98+%, S-type, 20 nm, polyhedral) were purchased from US Research Nanomaterials, Inc. The PU foam material was composed of two commercially reactants: component A and component B in the form of liquid kindly supplied by Exxon Panah Co., Iran (SROC: semi rigid open cell polyurethane foam) without any commercial filler. The polyisocyanate employed was diphenylmethane diisocyanate (MDI, ρ =1.23 g cm^{-3}) as component A. Component B consists of polyol (based on polyether,ρ = 1.1 g cm^{-3}), blowing agent, catalyst, and surfactant. Polyether polyols are extensively used for producing various polyurethanes, such as flexible, semi-flexible, and rigid foams [9]. Water is chosen as blowing agent.

3. Samples preparation

3.1. Preparation of blank PEUOC

The one-step system is currently used in the PEUOC foam fabrication [10]. For blank PU foam, two components mixed at a 1:1 ratio at 2000 rpm for about 10 s in an open cylindrical mould at room temperature. No heating was necessary. The polymerization reaction then takes place and simultaneously foaming begins due to CO_2 gas generation.

3.2. Preparation of PEUOC/MgO

Three different weight percentages of MgO NPs (1.0, 1.5 and 2.0 wt.%) were dissolved into polyol component solution individually using MS2 Minishaker IKA (Germany) for 20 s with 3000 rpm in an open cylindrical mould at room temperature until a homogenized solution was reached. Then MDI part was added to the solution by doing vortex at 2000 rpm for 10 s. As discussed [10], the preparation of foams is a simultaneous occurrence of

polymer formation and gas generation. For a well prepared sample and producing CO_2 gas during reaction time, the cover of the container of PEUOC/MgO was taken off. After 10–12 s reaction was ended by formation of foams in the samples. The ratio of polyol:MDI was 1 (2 ml):1 (2 ml) in all the synthesized samples. The procedure for fabricating PEUOC/MgO was similar to the procedure mentioned above. For the analysis purposes the samples were kept in the stream of the liquid nitrogen gas and then were cut in the slices with 1 mm diameter.

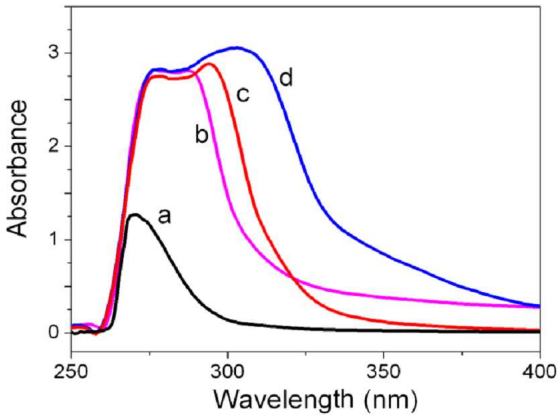

Fig. 1. UV-VIS absorption spectra of the PEU foams with MgO NPs content of (a) 0.0 wt.%, (b) 1.0 wt.%, (c) 1.5 wt.%, and (d) 2.0 wt.%.

The linear absorption spectra for all the compounds were obtained using UV–VIS spectrophotometer (PG Instrument UV-Visible system, model T80+) are shown in Fig. 1. The optical absorption spectrum has been recorded from 100 to 600 nm for blank PEUOC and PEUOC/MgO nanocomposites dissolved in N,N-dimethylformamide (DMF).

4. Results and discussion

In this section, the PU foams characterizations are studied and discussed via optical and SEM micrographs, and measurement of nonlinear optical properties via Z-scan technique results.

4.1. Optical micrographs

In order to determine the cell size of PEUOC/MgO foams and observing its microstructure, optical microscope is used. For this aim, thin layers of the synthesized samples were cut with a sharp razor blade into circular slices with 10 mm diameter and 1 mm thickness. The freeze-fractured surfaces of all the synthesized samples were obtained at liquid nitrogen temperature and then were examined. Optical micrographs were taken using an optical microscope (Nikon; TE 2000-S) in transmission mode with 40× magnification. All optical micrographs were provided from the surface perpendicular to the foaming direction.

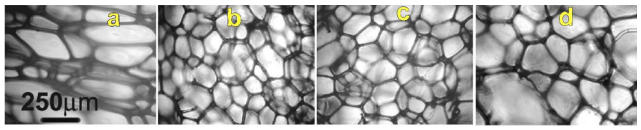

Fig. 2. Optical micrographs of the PEU foams with MgO NPs content of (a) 0.0 wt.%, (b) 1.0 wt.%, (c) 1.5 wt.%, and (d) 2.0 wt.%.

Figure 2 shows the transmission optical microscopy images of PEUOC including MgO NPs. Accordingly, by adding NPs in blank PEUOC the mean cell sizes in the matrix have been changed since PEUOC/MgO nanocomposites have smaller cell size in comparison with blank PEUOC. Figure 2a–d shows that the mean cell size of the foams decreases on the addition of MgO NPs from 0.0 wt.% up to 2.0 wt.%.

4.2. SEM analysis

Resulting samples are analyzed under a FESEM in different magnifications. Images are provided under a FESEM Hitachi (Japan) s4160 model using 30 kV accelerating voltage after coating the samples with a thin layer of gold. All foam pictures are taken perpendicular to the foam rising direction.

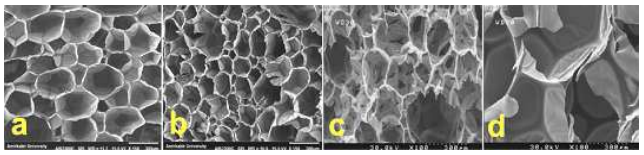

Fig. 3. SEM images of the PEU foams with (a) 0.0 wt.%, (b) 1.0 wt.%, (c) 1.5 wt.%, and (d) 2.0 wt.% MgO NPs.

The synthesized samples are analyzed under a FESEM in different magnifications. Figure 3 clearly reveals differences between PEUOC nanocomposites in the case of different loadings of NPs in macroscopic view. By increasing MgO NPs contents from 0.0 wt.% to 1.0 wt.% into PEUOC matrix, the cell sizes of the synthesized samples have decreased but by increasing MgO NPs contents from 1.0 wt.% to 2.0 wt.% into polymer matrix the cell sizes of the synthesized samples have increased.

Here, only the SEM images of nanocomposite foams with MgO NPs contents of 2.0 wt.% is shown in Fig. 4. The cell struts reveals that the PEUOC/MgO nanocomposite foams have microporous skeleton. As it is seen in Fig. 4a–e, close inspection (with 100×, 300×, 1k×, 6k×, and 30k× magnifications, respectively) of the strut cross-section shape in the cell structure of PEUOC foams that is concave equilateral triangular cross-section [10]. The presence of the microvoids can be explained in terms of the chemical reactivity of NPs with the isocyanate monomer [11]. Presence of NPs in a microvoid of foams gives evidence of the mentioned claim.

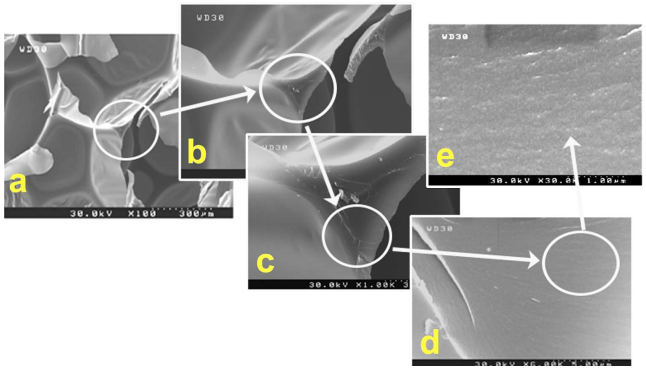

Fig. 4. SEM images of PEU nanocomposite loaded with 2.0 wt.% MgO NPs with different magnification, (a) 100×, (b) 300×, (c) 1k×, (d) 6k×, and (e) 30k× to show micro voids.

According to Fig. 4e, MgO NPs in the struts of foam skeleton are pulling out of the fracture surface to form interconnecting bridge structures between polymer/NPs interfaces, facilitating a load transfer mechanism for MgO NPs reinforcement of polymers [12].

4.3. Z-scan setup

The experimental setup for the Z-scan experiment is shown in Fig. 5. An incident laser beam from a CW Nd:YAG laser at its second harmonic frequency of 532 nm with TEM_{00} Gaussian profile which is propagating and focused by a lens ($f = 5$ cm) illuminating the sample. The radius of the beam waist ω_0 was determined by edge scan method as 37 μm.

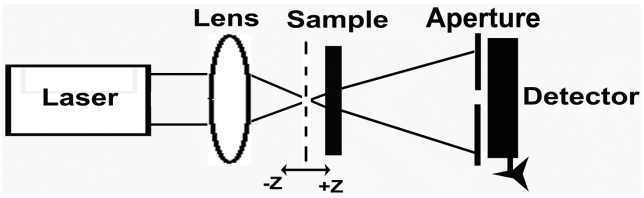

Fig. 5. Experimental setup for the close aperture Z-scan technique.

The sample is moved along the z axis in the vicinity of the focal plane of lens (the $+z$ direction is the laser propagation direction) [13]. The transmitted intensity is collected and recorded by a photodiode detector.

4.3.1. Z-scan theories on nonlinear process

Dependent intensity on the NLR and NLA are expressed by the equations

$$n(I) = n_0 + n_2 I, \tag{4.1}$$

$$\alpha(I) = \frac{\alpha_0}{1 + I/I_\mathrm{s}}, \tag{4.2}$$

where n_0 is the linear refractive index, n_2 is the NLR index, α_0 is the linear absorption coefficient, I is the intensity of the laser beam and I_s is the saturation intensity, respectively. In the case of $I/I_\mathrm{s} \ll 1$, Eq. (4.2) turns to $\alpha(I) = \alpha_0 + \beta I$ in which β is the NLA coefficient [14–17].

Z-scan is a simple but sensitive single-beam method for determining both of the magnitude and sign of NLR index, n_2, and NLA coefficient, β, of a given material by close and open aperture, respectively [18].

In this technique, a polarized Gaussian laser beam is focused on a narrow waist. The samples moved along z-direction through the beam focus ($z = 0$), self-focusing (positive) or self-defocusing (negative) modifies the wave front phase, thereby modifying the detected beam intensity [14].

For the close aperture condition the normalized transmission is given by [18–20]:

$$\Delta T_{\mathrm{p-v}} = 0.406(1 - S)^{0.25}(2\pi/\lambda) n_2 I_0 L_\mathrm{eff}, \tag{4.3}$$

where $\Delta T_{\mathrm{p-v}}$ is the difference between the normalized peak transmittance and valley transmittance, S is the aperture's linear transmittance, $L_\mathrm{eff} = [1 - \exp(-\alpha L)]/\alpha$ is the effective thickness of the sample, $I_0 = 2P_\mathrm{in}/\pi\omega_0^2$ is the incident intensity at focal point that is 2493.7 W/cm^2 and P_in is the laser power that is 55 mW in this work [5, 19, 20]. The linear absorption, α in low incident powers can be found from the following equation [17, 21]:

$$\alpha = -\frac{1}{L} \ln\left(\frac{P}{P_0}\right). \tag{4.4}$$

The values of α for different compositional percentages of MgO NPs in PEUOC are listed in Table.

TABLE

Z-scan data and calculated values of nonlinear optical properties of synthesized samples.

Sample	α [cm^{-1}]	$L_\mathrm{eff}[mm]$	ΔT	$n_2 \times 10^{-8}$ [cm^2/W]	$\beta \times 10^{-5}$ [cm/W]
blank PEUOC	0.1106	0.99449	0.032268	0.292568	2.48
PEUOC/1%MgO	0.975522	0.49771	0.05686	0.525561	8.9
PEUOC/1.5%MgO	0.978462	0.437063	0.083702	0.771339	11.2
PEUOC/2%MgO	0.986388	0.27474	0.192634	1.760913	17.2

In open aperture, it can be seen that aperture was replaced by a lens to collect all the light into power meter detector. The normalized transmittance of a nonlinear medium for open aperture z-scan is a function of β is given by

$$T_\mathrm{norm}(z) = \ln(1 + q_0(z,t))/q_0(z,t), \tag{4.5}$$

where $q_0(z,t) = \beta I_0 L_\mathrm{eff}/(1 + z^2/z_0^2)$, $z_0 = k\omega_0^2/2$ is the diffraction length of the beam, and $k = 2\pi/\lambda$ is the wave vector [18–20].

4.3.2. Close and open aperture Z-scan result

According to typical preparation procedure for Z-scan method, blank PEUOC and PEUOC/MgO nanocomposites have been dissolved into DMF, separately, since the solutions with 0.1 M were achieved. The samples were placed in a 1 mm thick quartz cell. In Z-scan experiment, the sample was moved forward or backward along the direction of the laser beam around the focus. The CA ($S = 0.32$) scheme allowed to determine both of the sign and the magnitude of n_2.

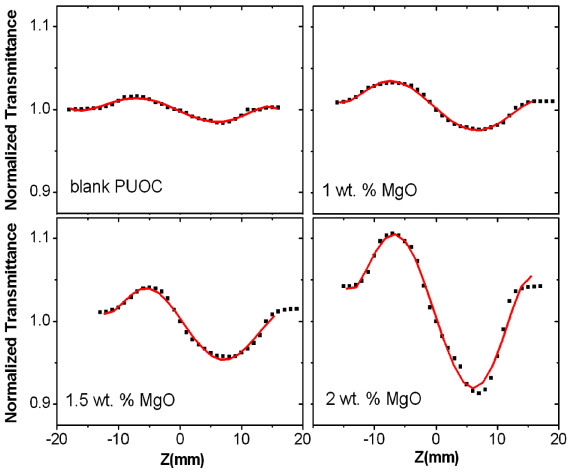

Fig. 6. Close aperture Z-scan experimental curves of PEUOC/MgO nanocomposite.

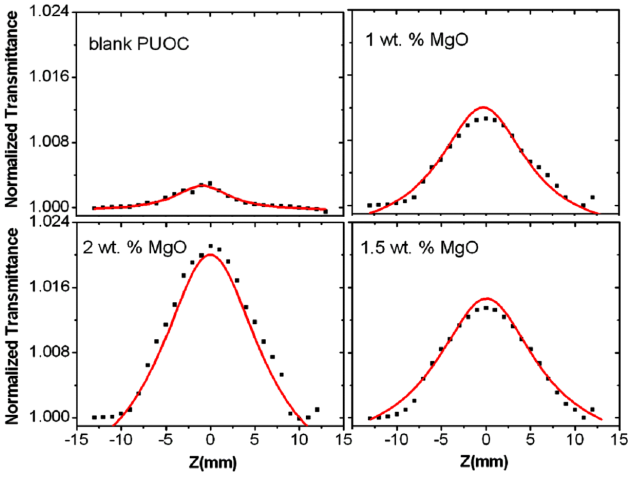

Fig. 7. Open aperture Z-scan experimental curves of PEUOC/MgO nanocomposites (normalized transmittance versus distance of focal length).

Close aperture Z-scan results of PEUOC/MgO. Figure 6 shows pure closed Z-scan data of different compositional percentages of MgO NPs in blank PEUOC. As it can be seen in the normalized curves of CA Z-scan exists a pair of peak and deep valley which can be identified as a self-defocusing material [19]. Since the valley comes after the peak of the transmittance, the sign of the refractive nonlinearity of all foams are negative that it shows self-defocusing effect of the synthesized samples. The order of NLR indices coefficients are 10^{-8} cm^2/W with negative sign that were obtained from Eq. (4.3) and is tabulated in Table.

The optical nonlinearity of aqua samples applied with CW laser beam is usually contributed to thermo-optical (thermal) effect. However, because of using the CW laser it is expectable that we detect thermal effects in the samples. Furthermore, by considering related research, it is more probability that thermal effect occurs for linear absorption which it is about 1 cm^{-1} [20]. This estimate confirms the theoretical and general estimate which made by other researchers [21–25].

Open aperture Z-scan results of PEUOC/MgO. It is seen that the OA transmittance is symmetric with respect to the focus ($z = 0$), where has a maximum transmittance. Figure 7 shows the OA Z-scan curves obtained for all synthesized samples. The values of β (cm/W) can be obtained from Eq. (4.5).

The NLA coefficients of the synthesized samples were obtained from OA Z-scan in the order of 10^{-5} (cm/W) with positive sign that shows the presence of strong saturable absorption (SA) [25]. It is clear that by adding MgO NPs into polymer matrix, the amount of β has increased. As a result, by adding NPs into blank PEUOC from 1.0 wt.% to 2.0 wt.% the NLR indices and the NLA coefficients of synthesized samples increased gradually. By adding MgO NPs into blank PEUOC, the polarity of system will be increased that tends to rising of the NLO properties.

By controlling the optimum ratio of MgO into PEUOC, it can be suggested as a promising and helpful candidate for applications in real optical systems by controlling the amount of NPs the nonlinear coefficients of samples can be adjusted. All the results of nonlinear absorption are calculated and displayed in Table.

5. Conclusions

PEUOC hybrids prepared by using *in situ* polymerization method with MgO NPs at loading fractions from 0.0 wt.% to 2.0 wt.% NPs. The third-order optical nonlinearities of PEUOC/MgO nanocomposites, dissolved in DMF are characterized by Z-scan technique with CW Nd:YAG laser at its second harmonic frequency of 532 nm as a light source. The new compounds exhibit good optical limiting properties at the wavelength used. The results conclude that it is promising candidate for the future optical device applications. The following results can be pointed:

- By evaluating optical micrographs of the synthesized foams, it is observed that the cell sizes of the samples have decreased by adding NPs into blank PEUOC.
- Considering SEM imaging, by increasing MgO NPs contents from 0.0 wt.% to 1.0 wt.% into PEUOC matrix, the cell sizes of the synthesized samples have decreased but by increasing MgO NPs contents from 1.0 wt.% to 2.0 wt.% into polymer matrix the cell sizes of the synthesized samples have increased.
- The nonlinear refractive index of the samples was obtained from CA Z-scan in the order of 10^{-8} (cm^2/W) with negative sign. By adding NPS into polymer matrix, the nonlinear refractive index has increased.

- The nonlinear absorption coefficients of the samples were obtained from OA Z-scan in the order of $10-5$ (cm^2/W) with positive sign. By adding NPs into polymer matrix, the amount of β is increased. The origin of β is the presence of strong saturable absorption (SA) effect.

References

[1] E. Chirackal Varkey, K. Sreekumar, *J. Appl. Polym. Sci.* **119**, 111 (2011).

[2] J. Sun, Q. Ren, X.Q. Wang, G.H. Zhang, D. Xu, *Opt. Laser Technol.* **41**, 209 (2009).

[3] F.Z. Henari, A.A. Dakhel, *J. Appl. Phys.* **108**, 1 (2010).

[4] Y. Sui, J.X. Lu, J. Yin, D. Wang, Z.K. Zhu, Z.G. Wang, *J. Appl. Polym. Sci.* **85**, 944 (2002).

[5] F.Z. Henari, A.A. Dakhel, *J. Appl. Phys.* **104**, 033110 (2008).

[6] E.W. Van Stryland, M. Sheik-Bahae, in: *Characterization Techniques and Tabulations for Organic Nonlinear Materials*, Eds. M.G. Kuzyk, C.W. Dirk, Marcel Dekker, 1998, p. 655.

[7] M.Y. Kariduraganavar, S.M. Tambe, R.G. Tasaganva, A.A. Kittur, S.S. Kulkarni, S.R. Inamdar, *J. Mol. Struct.* **987**, 158 (2011).

[8] Y. Zhang, M. Ma, X. Wang, D. Fu, H. Zhang, N. Gu, J. Liu, Z. Lu, L. Xu, K. Chen, *J. Phys. Chem. Solids* **64**, 927 (2003).

[9] K. Ashida, *Polyurethane and Related Foams: Chemistry and Technology*, Taylor and Francis Group, New York 2007.

[10] O. Doutres, N. Atalla, K. Dong, *J. Appl. Phys.* **110**, 064901 (2011).

[11] S. Basirjafari, R. Malekfar, S. Esmaielzadeh Khadem, *J. Appl. Phys.* **112**, 104312 (2012).

[12] C. McClory, T. McNally, G.P. Brennan, J. Erskine, *J. Appl. Polym. Sci.* **105**, 1003 (2007).

[13] S. Li Guo, B. Gu, T. Zhang, *J. Nonlinear Opt. Phys. Mater.* **13**, 45 (2004).

[14] K.K. Nagaraja, S. Pramodini, A. Santhosh Kumar, H.S. Nagaraja, P. Poornesh, D. Kekuda, *J. Opt. Mater.* **35**, 431 (2013).

[15] L. Chen, R. Hu, J. Xu, S. Wang, X. Li, S. Li, G. Yang, *J. Spectrochim. Acta A* **105**, 577 (2013).

[16] M.H. Majlesara, Z. Dehghani, R. Sahraei, A. Daneshfar, Z. Javadi, F. Divsar, *J. Quant. Spectrosc. Radiat. Transfer* **113**, 366 (2012).

[17] M. Sheik-Bahae, A.A. Said, T.H.E. Wei, D.J. Hagan, E.W. Van Stryland, *IEEE J. Quantum. Electron.* **26**, 760 (1990).

[18] M. Sheik-Bahae, A.A. Said, E.W. Van Stryland, *J. Opt. Lett.* **14**, 955 (1989).

[19] N. Qiu, D. Liu, S. Han, X. He, G. Cui, Q. Duan, *J. Photochem. Photobiol. A* **272**, 65 (2013).

[20] E.W. Van Stryland, M. Sheik-Bahae, A.A. Said, D.J. Hagan, *Prog. Cryst. Growth Charact.* **27**, 279 (1993).

[21] F. Wu, W. Tian, W. Chen, G. Zhang, G. Zhao, S. Cao, W. Xie, *J. Mod. Opt.* **56**, 1868 (2009).

[22] R.W. Boyd, *Nonlinear Optics*, Academic Press, New York 2007.

[23] S. Pramodini, P. Poornesh, K.K. Nagaraja, *Curr. Appl. Phys.* **13**, 1175 (2013).

[24] D.H.G. Espinosa, R.K. Onmori, *Phys. Procedia* **28**, 33 (2012).

[25] B.J. Rudresha, B.R. Bhat, D. Ramakrishna, J.K. Anthony, H.W. Lee, F. Rotermund, *Opt. Laser Technol.* **44**, 1180 (2012).